

## Preparation of nanofluid-based Coolanol-20 containing carbon nanotubes and validation of its efficiency in enhancing thermal conductivity

A. D. To<sup>b,c,\*</sup>, N. M. Phan<sup>a,b</sup>, H. T. Bui<sup>a,b</sup>

<sup>a</sup>*Institute of Materials Science (IMS), Vietnam Academy of Science and Technology (VAST), A2 Building, 18 Hoang Quoc Viet Street, Cau Giay District, Hanoi 122102, Viet Nam*

<sup>b</sup>*Graduate University of Science and Technology (GUST), Vietnam Academy of Science and Technology (VAST), 18 Hoang Quoc Viet Street, Cau Giay District, Hanoi, Viet Nam*

<sup>c</sup>*Vietnam National Space Center, Vietnam Academy of Science and Technology (VAST), 18 Hoang Quoc Viet Street, Cau Giay District, Hanoi, Viet Nam*

In this paper, we present the results obtained in the manufacturing and testing process of the thermal properties of nanofluid-based Coolanol-20 containing carbon nanotubes (CNTs). The presence of CNTs has improved thermal conductivity of the liquid, with a concentration of 1.0% vol CNTs showing an increase in thermal conductivity of 65%. To test the efficiency of the fluid, we have built a satellite model and a system that simulates the real working conditions of the satellite in space. Through our experiments, we have shown that Coolanol-20/CNTs has helped to improve heat exchange efficiency for components operating under harsh conditions.

(Received November 4, 2021; Accepted February 8, 2022)

*Keywords:* Coolanol-20, CNTs, Thermal conductivity, Nanofluid, Heat exchange, Satellite, PFL

### 1. Introduction

Thermal control plays an important role in improving stability, durability and longevity of electronic components and devices. Currently, there are many technologies and techniques in heat dissipation, among which the liquid cooling method is applied to heat-generating electronic components and devices [1]. Liquid cooling technology is receiving great attention from researchers, engineers and is applied in different kinds of equipment due to its fast heat-exchange capacity and reasonable prices. However, common cooling fluids such as water, ethylene glycol (EG), propylene glycol (PG) and oil often have poor thermal conductivity, so there is a certain limit to improving heat dissipation efficiency. Recently, researchers have introduced into liquids some solid nano-sized materials to improve thermal conductivity of traditional liquids, thereby improving and enhancing their heat transfer efficiency [2]. As a result, a new fluid, called nanofluid (NF), was created and developed, whose definition is a liquid containing nanometer-sized particles including metal nanoparticles (Cu, Au, Ag, Ni); metal oxides ( $\text{Al}_2\text{O}_3$ , CuO,  $\text{Fe}_2\text{O}_3$ ,  $\text{SiO}_2$ ,  $\text{TiO}_2$ ); or ceramic (SiC, AlN, SiN) [3]. Nanofluids have much greater thermal conductivity and heat transfer efficiency than previously used traditional liquids.

Carbon nanotubes are known to be one of the materials with the highest thermal conductivity known ( $\text{kCNTs} = 2,000 \text{ W/mK}$ ), which has opened up a new research direction for applications of this material in liquid cooling technology [4]. A large number of studies have been conducted, but most of them have focused on the applications of CNTs in base fluids that are distilled water, EG, PG or a mixture of them [5-8]. These fluids have a rather narrow operating temperature range, while electronic devices operating in harsh environments such as space require a wider operating temperature range [9]. One of the fluids frequently used for thermal control of equipment operating in harsh environments is Coolanol-20 [10], with an operating temperature ranging from  $-101^\circ\text{C}$  to  $149^\circ\text{C}$ . However, studies on Coolanol-20 base liquid containing CNTs

---

\* Corresponding author: [taduc@vnsr.org.vn](mailto:taduc@vnsr.org.vn)  
<https://doi.org/10.15251/DJNB.2022.171.193>

have not been performed so far. Therefore, in this paper, we present the results obtained in the manufacturing and testing process of thermal properties of Coolanol-20 base fluid containing CNTs.

## 2. Experiment

### 2.1. Materials

CNTs materials with diameters between 20 - 80 nm, and 98% purity were fabricated by the thermal CVD method at Institute of Materials Science (IMS). Coolanol-20 base fluid was purchased from ExxonMobil. The chemicals used in the modification of CNTs and dispersions were  $H_2SO_4$ ,  $HNO_3$ ,  $SOCl_2$ ,  $H_2O_2$  and Tween-80, purchased from Sigma-Aldrich.

### 2.2. Fabrication of the nanofluid

In order to improve the dispersion of CNTs into the base fluid, the surface of the CNTs materials needs to be modified to attach chemical functional groups. The process of modifying CNTs with functional groups -OH is presented in Figure 1. First, CNTs are functionalized with carboxyl functional groups (-COOH) by a mixture of  $HNO_3:H_2SO_4$  acids (corresponding volume ratio 1:1) at  $70^\circ C$  for 5 hours. The product obtained after functionalization is filtered with distilled water, then CNTs-COOH is dispersed in  $SOCl_2$  solution and stirred continuously for 24 hours at  $60^\circ C$  to obtain the CNTs-COCl materials. CNTs-COCl materials after being cleaned with distilled water are filtered and washed with  $H_2O_2$  to form CNTs-COOH materials.

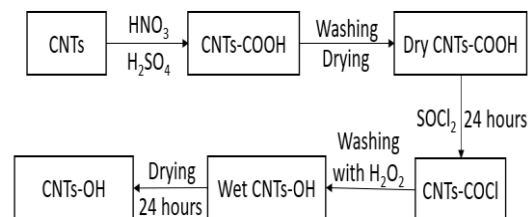


Fig. 1. Process for denaturing CNTs-OH.

To disperse carbon nanoparticles into liquid, we use the dispersion process described in Figure 2. In this process, CNTs are modified to attach -OH functional groups as shown above, then CNTs-OH is uniformly dispersed into the Coolanol-20 base fluid by using Tween-80 surfactant combined with using an ultrasonic vibration device for 30 - 90 minutes.

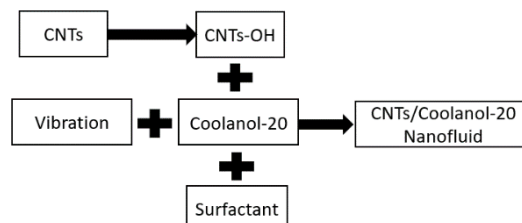


Fig. 2. Process of dispersing CNTs in liquid.

### 2.3. Analytical measurements

The morphology of the samples was investigated using a field-effect scanning electron microscope (FESEM, Hitachi S4800). The functional groups were analyzed by an infrared

spectroscopy (Prestige 21-SHIMADZU FTIR spectrometer) in the range of wave numbers from 1000 to 4000  $\text{cm}^{-1}$ . Raman scattering spectra was measured with an iHR550 Jobin-Yvon instrument under the excitation wavelength of Ar laser of 514 nm. Nanofluids were evaluated for dispersion and stability using a ZetaSizer instrument. The thermal conductivity of the nano fluid was measured with a Transient Hot Bridge THB-100 device.

### 3. Results and discussions

Figure 3 shows the surface morphology of CNTs examined by SEM technique with a magnification of 200,000 times. The image shows that CNTs have a fibrous structure with a diameter distribution in the range of 20 nm - 80 nm and have high cleanliness as there is no existence of dirty impurities such as amorphous carbon components.

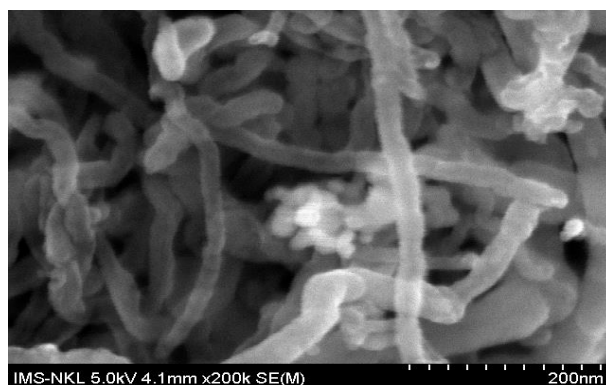


*Fig. 3. SEM image of CNTs material.*

Results of FTIR and Raman spectra of CNTs, CNTs-COOH, and CNTs-OH have been published by authors in previous works [11-12]. The results of Raman spectroscopy of CNTs, CNTs-COOH and CNTs-OH show a D peak at wave number 1351  $\text{cm}^{-1}$  and a G peak at wave number 1591  $\text{cm}^{-1}$  in the spectrum of all samples. However, the ratio of peak intensity D to peak intensity G ( $I_D/I_G$ ) were different for different samples. The  $I_D/I_G$  ratio of CNTs-OH is highest (1.87) because in order to functionalize with the -OH functional group, the sample has been treated with strong acid twice, resulting in many defects in the obtained sample, making the  $I_D/I_G$  ratio high. Meanwhile, the  $I_D/I_G$  ratio of the CNTs-COOH sample is 0.99 and that of the CNTs sample is the lowest, which is 0.79. The FTIR spectral results show some characteristic peaks of the bonds, among which the peak around the wave number 3431  $\text{cm}^{-1}$  is caused by the vibration of the -OH group, and this region is more extended for CNTs-COOH and CNTs-OH. The peak around the wave number 1624  $\text{cm}^{-1}$  is due to the vibration of the C=C bond of the graphite lattice in the structure of CNTs. For CNTs-COOH, peaks appear around 1728  $\text{cm}^{-1}$  and 1581  $\text{cm}^{-1}$ , corresponding to the vibrations of C=O and C-O bonds of the carboxyl group. The above characteristic peaks are no longer found in the CNTs-OH sample, and this is because the -OH functional groups have completely replaced the positions of the -COOH groups on the surface of CNTs. Thus, the results show that the process of denaturing -COOH and -OH functional groups has been successful on the surface of CNTs.

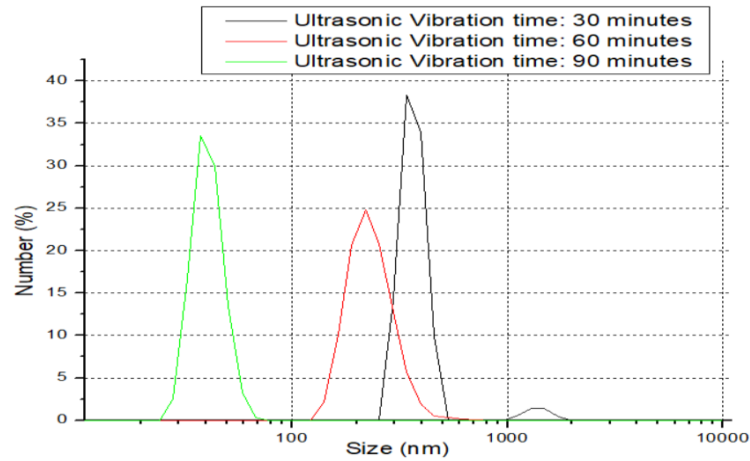


Fig. 4. Results of CNTs distribution by size in liquid with ultrasonic vibration time: 30 minutes, 60 minutes and 90 minutes.

Figure 4 is the results of the size distribution of CNTs in the Coolanol-20 fluid with different ultrasonic vibration times of 30 minutes, 60 minutes and 90 minutes. The result with ultrasonic vibration time of 30 minutes shows the existence of two peaks of 320 nm and 1.6  $\mu\text{m}$ , which confirm the clustering of CNTs in the liquid. With the ultrasonic vibration time of 60 minutes, it shows that CNTs have better dispersion with the appearance of only a single peak of 240 nm. However, the dispersion result is not satisfactory and still converges because the size of CNTs in the range of 20 – 80 nm does not match the 240 nm peak. The dispersion result with a time of 90 minutes shows that the size of CNTs is distributed in the range of 16 nm - 80 nm. This range is consistent with the size of CNTs in the range of 20 - 80 nm, which shows that the ultrasonic vibration time of 90 minutes is required to achieve uniform dispersion of CNTs in the Coolanol-20 base fluid.

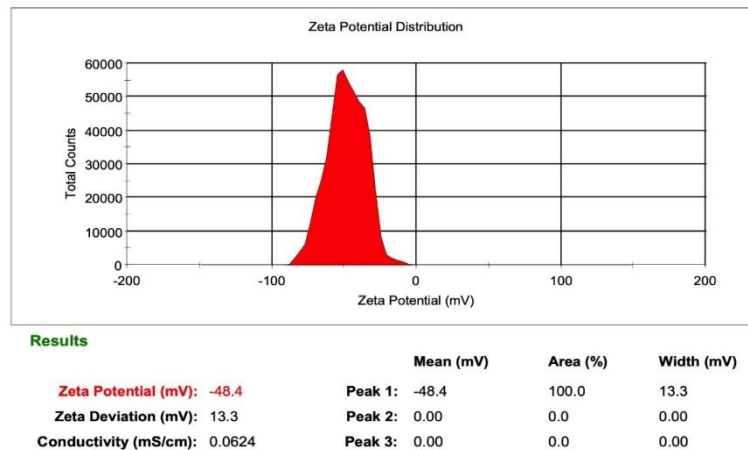


Fig. 5. Zeta potential results of Coolanol-20-based nanofluid containing CNTs.

Figure 5 is the result of zeta potential of Coolanol-20-based nanofluid containing CNTs with a measured value of 48.4 mV. The Zeta potential in the range  $\pm 40$  mV to  $\pm 60$  mV indicates that CNTs have a stable dispersion in the Coolanol-20 base fluid.

The increase in thermal conductivity of the Coolanol-20-based nanofluid containing CNTs-OH is shown in Figure 6. The increase of the thermal conductivity coefficient is calculated according to the formula:

$$\%k = [(k - k_0) \times 100] / k_0 \quad (1)$$

where  $k_0$  is the thermal conductivity of Coolanol-20;  $k$  is the thermal conductivity of the nanofluid in the presence of CNTs.

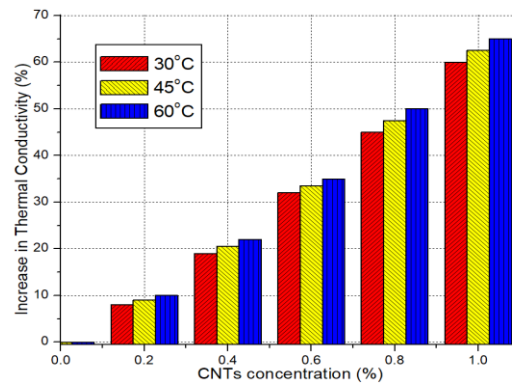


Fig. 6. The increase in thermal conductivity of the Coolanol-20-based nanofluid containing CNTs-OH.

From Figure 6, it can be seen that the samples all have increasing thermal conductivity as the CNTs concentration and temperature increase. The increase in thermal conductivity of the nanofluid with temperature can be explained by Li et al. [13]. Li reported that the Brownian motion as well as the change in agglomeration of nanocomponents and viscosity with temperature are important factors affecting thermal conductivity of liquids [13]. According to Li, an increase in temperature leads to the following effects: (i) reduced clustering of nanocomponents due to a decrease in surface energy; (ii) enhanced Brownian motion due to a decrease in viscosity [10]. The enhancement of the Brownian motion is the basis for the increase in thermal conductivity of the liquid with increasing temperature. Figure 6 compares the increase in thermal conductivity of different liquids at 30°C and 60°C, showing that at higher temperatures, thermal conductivity increases. With the concentration of 1.0% vol of CNTs-OH at 30°C, we see that the thermal conductivity of the nano fluid has an enhancement of 59%. The thermal conductivity of the nano fluid reached the maximum value of 65%, corresponding to the CNTs content of 1.0% vol and temperature of 60°C.

#### 4. Validation

In order to perform the testing of the base fluid containing CNTs that we have fabricated, we have cooperated with Vietnam National Space Center (VNSC) to design and manufacture a satellite model in the laboratory to study its thermal control process.

In our experiment, the satellite model is placed in a vacuum chamber with a pressure of  $10^{-4}$  bar to ensure that there is no heat transfer phenomenon (in order to simulate the space environment). On one side of the vacuum chamber, a light source with a strong heat-emission capacity is installed to simulate sunlight during the day (emission power from 0 - 7.5 kW/m<sup>2</sup>) so that the surface temperature of the side facing the light source can reach a peak of 100°C. The opposite side of the vacuum chamber is installed with a liquid nitrogen chamber to simulate the case of low temperatures at night (the lowest temperature could reach -75°C). The conditions of the operating environment of the satellite model will be altered in real time to be as close as possible to the actual environmental conditions of a corresponding satellite in space. In this simulation, we have chosen the Pumped Fluid Loop (PFL) as the method for thermal control. The model of the entire system used to simulate the thermal control process is shown in Figure 7.

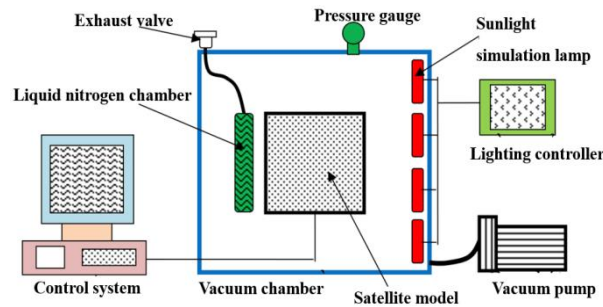


Fig. 7. Vacuum chamber model used to simulate the thermal control process using nanofluids containing CNTs.

The PFL uses Coolanol-20 base fluid containing CNTs with concentrations varying from 0.2% to 1.0% to test the efficiency of the thermal control in two hypothetical situations:

**a) Dissipating heat of a satellite component to the satellite shell**

In this situation, we assume that there is a balance between the incoming thermal radiation and the outgoing thermal radiation, corresponding to the saturation temperature of the satellite shell being 25°C. The heat from a component with capacity  $P = 10$  W will be radiated through the satellite shell to space environment. The simulation test results in Table 1 show that after about 43 minutes, the temperature of the component reaches the saturation value, and this value decreases by 4.2°C when using 1% CNTs.

Table 1. Results in the first hypothetical situation.

Volume (%)	Saturation time (minutes)	Saturation temperature when using Coolanol/CNTs (°C)
0.0	43.0	62.6
0.2	43.0	61.8
0.4	43.5	60.9
0.6	44.0	60.0
0.8	44.0	59.1
1.0	44.5	58.4

**b) Taking heat from hot a component to warm a cold device**

In this situation, we assume the satellite operates in the absence of sunlight and the temperature of the surrounding space is at about -75°C. Heat from the hot component instead of radiating directly to the satellite shell will be used to warm the hypothetical camera block, which needs a stable operating temperature range. The simulation test results in Table 2 show that in this situation, the satellite shell and outer surface of the camera have a temperature of about 12°C. After about 32 minutes, the temperatures of the hot component and the camera reaches the saturation values. It is also noticeable that we achieve the best heat dissipation performance for the satellite component and heating for the camera when the base fluid contains CNTs concentration of 1%.

Table 2. Results in the second hypothetical situation.

CNTs (%)	Temperature of the body shell (°C)	Saturation time (minutes)	Saturation temperature of the chip (°C)	Saturation temperature of the camera (°C)
0.0	12.2	32.0	49.4	20.5
0.2	12.5	32.0	48.8	21.5
0.4	12.3	32.5	48.2	23.0
0.6	12.8	32.5	47.4	23.7
0.8	12.7	33.0	46.6	24.3
1.0	12.6	33.0	45.9	24.5

The above test results have shown that Coolanol-20 containing CNTs is effective and has great potential for application in thermal control for satellites, helping to improve efficiency, stability, durability as well as their lifetime during operation.

## 5. Conclusions

CNTs material was successfully modified with -OH functional group to disperse into Coolanol-20 base fluid. By using the ultrasonic vibration method combined with surfactant, CNTs-OH was uniformly dispersed into the liquid. The Zeta measurement revealed the stability of CNTs-OH in the base fluid. The thermal conductivity of the Coolanol-20 base fluid containing CNTs-OH material increased by 65% compared to that of the conventional liquid with 1.0% vol concentration of CNTs-OH at 60°C. After that, the Coolanol-20 base fluid containing CNTs-OH material was tested in two separate experiments and proved to be able to increase thermal conductivity of the PFL. Therefore, it has a great potential for thermal control of components in satellites that often operate under extreme conditions.

## Acknowledgements

The authors acknowledge financial support from National Foundation for Science and Technology Development (NAFOSTED) under project no. NCUD.01-2019.43.

## References

- [1] X. Q. Wang, A.S. Mujumdar, *International Journal of Thermal Sciences* 46, 1 (2007); <https://doi.org/10.1016/j.ijthermalsci.2006.06.010>
- [2] M. Raja, R. Vijayan, P. Dineshkumar, M. Venkatesan, *Renewable & Sustainable Energy Reviews* 64, 163 (2016); <https://doi.org/10.1016/j.rser.2016.05.079>
- [3] H. E. Patel, T. Sundararajan, S. K. Das, *Journal of Nanoparticle Research* 12, 1015 (2010); <https://doi.org/10.1007/s11051-009-9658-2>
- [4] A. K. Rasheed, M. Khalid, W. Rashmi, T. C. S. M. Gupta, A. Chan, *Renewable & Sustainable Energy Reviews* 63, 346 (2016); <https://doi.org/10.1016/j.rser.2016.04.072>
- [5] E. Sadeghinezhad, M. Mehrali, R. Saidur, M. Mehrali, S. T. Latibari, A. R. Akhiani, H. S. C. Metselaar, *Energy Conversion and Management* 111, 466 (2016); <https://doi.org/10.1016/j.enconman.2016.01.004>
- [6] Ghozatloo, M.S. Niasar, A. Rashidi, *International Communications in Heat and Mass Transfer* 42, 89 (2013); <https://doi.org/10.1016/j.icheatmasstransfer.2012.12.007>
- [7] V. T. Pham, N. A. Nguyen, H. T. Bui, D. Q. Le, T. H. Nguyen, M. H. Nguyen, H. K. Phan, N. M. Phan, N. H. Phan, *RSC Advances* 7, 318 (2017).

- [8] S. Baskar, M. Chandrasekaran, T. Vinod Kumar, P. Vivek, L. Karikalan, *International Journal of Ambient Energy* 41(3), 296 (2020); <https://doi.org/10.1080/01430750.2018.1451381>
- [9] C. R. Raj, S. Suresh, V. K. Singh, R. R. Bhavsar, S. Vasudevan, V. Archita, *International Journal of Thermal Sciences* 167, 107007 (2021); <https://doi.org/10.1016/j.ijthermalsci.2021.107007>
- [10] H. J. van Gerner, R. C. van Benthem, J. van Es, D. Shwaller, S. Lapensee, Fluid selection for space thermal control systems, *International Conference on Environmental Systems*, 13 (2014).
- [11] H. T. Bui, V. T. Pham, D. Q. Le, T. H. Nguyen, H. K. Phan, N. M. Phan, *Journal of the Korean Physical Society* 65(3), 312 (2014).
- [12] V. T. Pham, N. A. Nguyen, T. H. Nguyen, N. H. Phan, N. M. Phan, H. T. Bui, *Journal of Molecular Liquids* 269, 344 (2018).
- [13] Y. H. Li, W. Qu, J. C. Feng, *Chinese Physics Letters* 25, 3319 (2008); <https://doi.org/10.1088/0256-307X/25/9/060>